Incommensurate magnetic ordering in Ti-doped $Sr_3Ru_2O_7$

P. Steffens,[1,*] J. Farrell,[2] S. Price,[1] A. P. Mackenzie,[2] Y. Sidis,[3] K. Schmalzl,[4] and M. Braden[1,†]
[1]*II. Physikalisches Institut, Universität zu Köln, Zülpicher Str. 77, D-50937 Köln, Germany*
[2]*Scottish Universities Physics Alliance, School of Physics and Astronomy, University of St. Andrews, North Haugh, St. Andrews KY16 9SS, Scotland*
[3]*Laboratoire Léon Brillouin, CEA/CNRS, F-91191 Gif-sur-Yvette CEDEX, France*
[4]*IFF, Forschungszentrum Jülich GmbH, JCNS at ILL, 38042 Grenoble Cedex 9, France*
(Received 17 July 2008; published 20 February 2009)

Magnetic correlations in Ti-substituted $Sr_3(Ru_{1-x}Ti_x)_2O_7$ have been studied by elastic and inelastic neutron-scattering techniques. Below transition temperatures of the order of 20 K, the samples with 7.5 and 10% of Ti content exhibit an incommensurate spin-density wave ordering with a propagation vector $\mathbf{q_{ic}}=(0.24,0.24,0)$, which does not reflect the dominant magnetic instabilities in pure $Sr_3Ru_2O_7$. Strong inelastic correlations near $\mathbf{q_{ic}}$ were found to persist in $Sr_3(Ru_{1-x}Ti_x)_2O_7$ far above the magnetic ordering; they become gapped in the ordered state.

DOI: 10.1103/PhysRevB.79.054422 PACS number(s): 75.30.Fv, 75.25.+z, 75.30.Hx, 75.30.Kz

I. INTRODUCTION

Among the layered perovskite ruthenates, which exhibit a variety of exciting magnetic properties, the bilayer compound $Sr_3Ru_2O_7$ has attracted particular interest over the recent years due to the observation of quantum-critical behavior related to its metamagnetic transition.[1] The quantum-critical phenomena arise from a low-lying critical end point whose temperature may be suppressed by variation in the magnetic field direction.[2,3] Several aspects of the metamagnetic transition remain, however, poorly understood, such as the splitting into multiple transitions and the formation of a novel phase around the quantum-critical end point.[4,5]

Pure $Sr_3Ru_2O_7$ stays paramagnetic down to the lowest temperature but displays strong magnetic fluctuations, as evidenced by ^{17}O NMR and by inelastic neutron-scattering measurements.[6–9] These results clearly show that magnetic fluctuations of ferromagnetic and antiferromagnetic characters coexist; their ratio depends on the temperature and field range. While NMR measurements do not yield very detailed information about the Q dependence of the susceptibility $\chi(q)$, inelastic neutron-scattering experiments at low temperature and at zero field[7] reveal two-dimensional magnetic correlations peaked at incommensurate antiferromagnetic positions on the axes of the pseudotetragonal Brillouin zone: $(q_1,0,0)$ and $(q_2,0,0)$ and equivalent vectors with $q_1 \simeq 0.09$ and $q_2 \simeq 0.25$. The positions of these incommensurate magnetic correlations are remarkably similar to those in single-layered $Ca_{2-x}Sr_xRuO_4$ for $0.2<x<0.6$ (Refs. 10 and 11) which also exhibits a metamagnetic transition.

The reported enhancement of antiferromagnetic fluctuations near the critical field in $Sr_3Ru_2O_7$ is surprising insofar as the metamagnetic transition should intuitively rather correspond to a ferromagnetic instability. For instance, in the single-layer ruthenate $Ca_{1.8}Sr_{0.2}RuO_4$, it has been shown that indeed the ferromagnetic fluctuations become enhanced at the metamagnetic transition.[11] A better understanding of the role which the different magnetic instabilities play in the metamagnetism in $Sr_3Ru_2O_7$ is highly desirable.

In view of the apparently quite complicated interplay of different magnetic instabilities, the study of substitution effects can be a very helpful tool as chemical substitution may shift the balance and selectively enhance one of the instabilities. In the case of $Sr_3Ru_2O_7$, it has recently been demonstrated that doping with Ti or Mn on the Ru site induces interesting effects.[12,13] By only a few percent of Mn substitution, the ground state of $Sr_3Ru_2O_7$ becomes an antiferromagnetic insulator with the magnetic ordering described by a commensurate (0.25,0.25,0) propagation vector.[12] For Ti-substituted $Sr_3Ru_2O_7$, Hooper *et al.*[13] reported the suppression of the metamagnetic transition and the upturn of the low-temperature specific heat for low Ti content.

Ti doping has already been investigated in the single-layer[14–18] (Sr_2RuO_4) and in the perovskite[19–21] ($SrRuO_3$) compounds. Concerning the electronic configuration, it has been argued that the Ru $4d$ and the Ti $3d$ bands are well decoupled and that Ti is in its nonmagnetic 4+ state ($3d^0$). The Ti^{4+} ion has the same oxidation number and a similar ionic radius as Ru^{4+} and is easily incorporated in the crystal structure, where it acts as an impurity. The Ti^{4+} substitution decreases the average number of Ru neighbors, i.e., the effective Ru coordination, and thereby reduces the Ru $4d$-band widths. In Sr_2RuO_4 only a few percent of Ti doping is sufficient to freeze the dominant magnetic instability of the pure compound into a spin-density wave at the same q vector.[15,22]

We have studied Ti-doped $Sr_3Ru_2O_7$ by various neutron-scattering techniques. For the Ti concentrations of 7.5 and 10% we find an incommensurate spin-density wave magnetic ordering whose propagation vector, $\mathbf{q_{ic}}=(0.24,0.24,0)$, does not coincide with the incommensurate dynamic correlations in the pure compound.[7]

II. EXPERIMENTAL

Single crystals of $Sr_3(Ru_{1-x}Ti_x)_2O_7$ with the two Ti concentrations $x=7.5\%$ and $x=10\%$ have been grown by a floating zone technique. Neutron-scattering measurements were carried out on the 4F1 spectrometer at the LLB in Saclay and on the IN12 and IN22 spectrometers at the ILL in Grenoble. On 4F1, a configuration with $k_f=2.662$ Å^{-1} and two pyro-

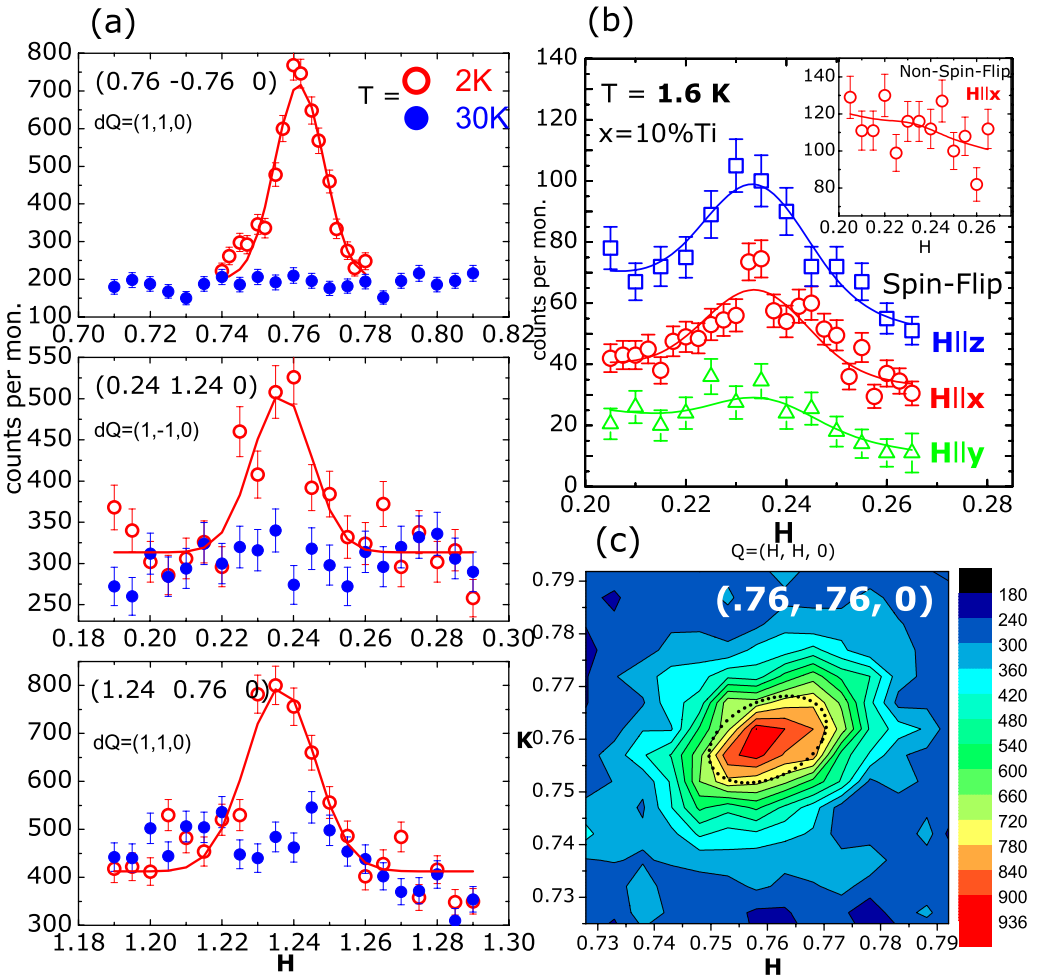

FIG. 1. (Color online) Elastic magnetic scattering in $Sr_3(Ru_{0.9}Ti_{0.1})_2O_7$. In (a) we show the intensity at various Q vectors at $T=2$ and 30 K. All three scans run in diagonal direction. (b) Summarizes the spin-flip count rates for the three polarization directions $H\|x,y,z$, together with the nonspin-flip count rate (inset) for $H\|x$ (inset). A mapping of the scattering around the (0.76,0.76,0) reflection in the H,K plane ($T=2$ K) is shown in (c). The dotted black ellipse indicates the resolution of the spectrometer.

lytic graphite (PG) filters has been used, and a standard polarized neutron setup allowed for a longitudinal polarization analysis of the scattering. On IN12, we worked with $k_f=1.5$ Å^{-1} and a Be filter, and a vacuum box around the sample allowed for a significant reduction in background at low scattering angles. While these experiments focused on the elastic scattering using small crystals with dimensions of a few millimeters, a large assembly of five coaligned $Sr_3(Ru_{0.9}Ti_{0.1})_2O_7$ crystals of about 500 mm^3 was studied by inelastic neutron scattering on IN22 ($k_f=2.662$ Å^{-1}; PG filter). Throughout the paper, we index all wave vectors in reduced lattice units referring to the tetragonal unit cell, $a=b\simeq 3.9$ Å and $c\simeq 20.6$ Å. Specific-heat measurements were performed on a larger series of $Sr_3(Ru_{1-x}Ti_x)_2O_7$ single crystals ($x=0$, 0.005, 0.01, 0.025, 0.05, 0.075, and 0.1) using a ^{3}He device at the University of Edinburgh.[23] Resistivity was measured by a standard four-probe technique and magnetic susceptibility using a superconducting quantum interference device (SQUID) magnetometer.

III. STATIC SPIN-DENSITY WAVE ORDERING

By elastic neutron scattering at low temperature, superstructure reflections were searched by scanning along the high-symmetry directions of the Brillouin zone. No signal is observed along the $a^\star/b^\star$ axes, but along the diagonals of the Brillouin zone additional intensity appears at low temperature. In the $(Q_h,Q_k,0)$ plane we find superstructure scattering at *all* wave vectors which are displaced by $\mathbf{q}_{ic}=(\pm 0.24,\pm 0.24,0)$ from integer values $(H,K,0)$. Figure 1(a) shows a collection of such scans, proving the intensity appearing at these positions at low temperature. In contrast to the interpretation in Ref. 13, the character of the magnetic ordering in $Sr_3(Ru_{1-x}Ti_x)_2O_7$ is not ferromagnetic but a spin-density wave close to the commensurate quarter-indexed order of up-up-down-down configuration, which has been reported for Mn-doped $Sr_3Ru_2O_7$.[12]

To unambiguously establish the magnetic nature of these peaks, we have carried out a polarized neutron study on the 4F1 spectrometer. In this experiment, one measures the spin-flip and the nonspin-flip scatterings separately, and by the application of a small magnetic guide field, the spin direction of the neutron at the sample position can be chosen along any spatial direction. The longitudinal polarization analysis adds an additional selection rule to the general neutron-scattering law that only magnetic components perpendicular to the scattering vector $\vec{Q}$ contribute: in the spin-flip channel

the magnetic polarization must be perpendicular to the neutron polarization. In the notation of Fig. 1(b) and with the [110]/[001] scattering plane used in this experiment, the directions are defined such that x is parallel to the scattering vector, y is along [001], and $z \| [1\bar{1}0]$. Due to a small amount of a ferromagnetic $Sr_4Ru_3O_{10}$ [T_C=105 K (Ref. 24)] impurity phase, neutron depolarization effects were sizeable in this experiment and needed to be taken into account. When correcting for the finite polarization, the measured intensities for the different spin directions indicate a magnetic moment aligned along the crystallographic c direction.

Figure 1(c) contains a mapping of the (0.76,0.76,0) reflection for $Sr_3(Ru_{0.9}Ti_{0.1})_2O_7$. Fitting the widths of the peak at this and other positions to a Lorentzian peak function and taking into account the experimental resolution, we obtain an isotropic correlation length of 168 ± 5 Å in the a,b plane, which corresponds to about 40 lattice spacings. The in-plane correlation length is thus significantly larger than the mean Ti-Ti distance in a single layer. The in-plane correlation length was also determined for the $Sr_3(Ru_{0.925}Ti_{0.075})_2O_7$ sample where it amounts to only 60 ± 10 Å. The significantly reduced correlation length seems to reflect the less stable magnetic ordering at this composition which is seen in the reduced transition temperature as well as in the macroscopic properties.

When discussing the c axis correlation of the magnetic order in the bilayer compound, one has to distinguish the coupling within a double layer (intrabilayer) and that between the double layers (interbilayer). The former can be expected to be of comparable strength as the in-plane coupling whereas the interdouble-layer coupling should be much smaller. In view of the large in-plane correlation length one may expect the coupling between the two planes in a double layer to be rather perfect. The observation of the signal at $\vec{Q}=(0.24,0.24,0)$ directly proves an essentially ferromagnetic coupling in the double layer, which agrees with the magnetic order in $Ca_3Ru_2O_7$.[25] The stacking of the magnetically ordered double layers, however, seems to be limited to short range, as it can be seen in the q_l scans shown in Fig. 2. As mentioned above, intensity has been found in the $(Q_h,Q_k,0)$ plane at all wave vectors displaced by $\mathbf{q_{ic}}$ from any integer $(H,K,0)$ value. Due to the body centered structure, however, only $(H,K,0)$ with $H+K$ even are zone centers, while the others are three-dimensional zone boundaries associated with a phase shift between neighboring double layers. Figure 2(b) shows that for $\vec{Q}=(0.76,0.76,q_l)$ the intensity is maximum at $q_l=0$, while for $(1.24,0.24,q_l)$ it is maximum at $q_l=1$. Therefore, in both cases the magnetic satellite is found to be displaced by $\mathbf{q_{ic}}=(0.24,0.24,0)$ away from the three-dimensional Bragg positions [(1,1,0) and (1,0,1), respectively], which indicates a ferromagnetic coupling between the neighboring double layers. The q_l dependence of the magnetic signal in $Sr_3(Ru_{1-x}Ti_x)_2O_7$ can be fitted with the superposition of broad Lorentzian peak profiles whose half width at half maximum indicate a correlation length corresponding to an exponential decay of the order parameter of only ~12 Å. The stacking of the magnetically ordered layers is quite limited similar to the case of Ti-doped Sr_2RuO_4.[15] We emphasize that the magnetic ordering in

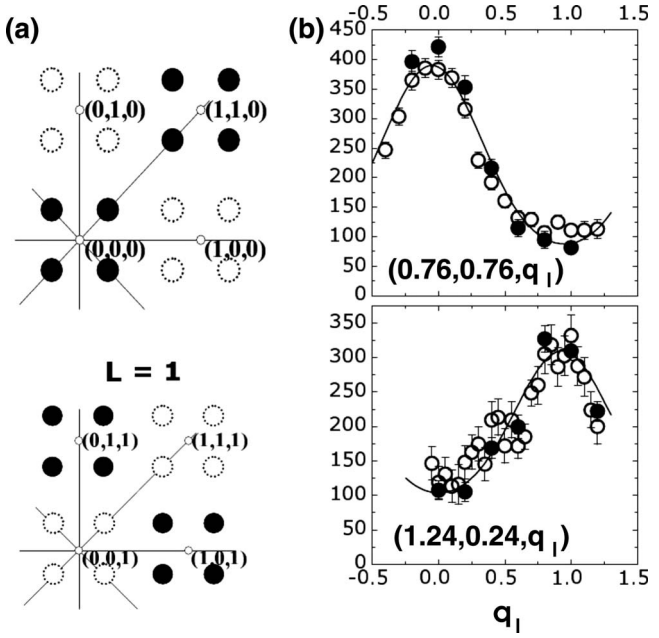

FIG. 2. q_l dependence of the magnetic intensity. In the sketches of the (hk0) and (hk1) planes (a) filled circles denote $\vec{Q}$ positions displaced by $\mathbf{q_{ic}}=(0.24,0.24,0)$ from a 3D-zone center, i.e., (0,0,0), (1,1,0), etc., whereas the open circles denote $\vec{Q}$ positions displaced by $\mathbf{q_{ic}}$ from a 3D-zone boundary, i.e., (0,1,0) and (1,0,0). The intensity at the latter positions is due to the large extensions of the scattering along c. The data in (b) show scans along q_l for two inequivalent values of H and K (open and closed symbols obtained in different scanning modes) referring to satellites around (1,1,0) and (1,0,1), respectively. In these plots, the background has been subtracted; i.e., any intensity is truly magnetic.

$Sr_3(Ru_{1-x}Ti_x)_2O_7$ cannot be considered as a three-dimensional phase transition due to the finite correlation lengths. Apparently the disorder induced by the Ti prohibits a well-defined transition.

Figure 3 summarizes the temperature dependence of the elastic magnetic scattering. For the sample with x=7.5% Ti we estimate the magnetic transition temperature by linearly extrapolating the temperature dependence of the magnetic scattering to $T_{\mathrm{mag}} \simeq 17$ K, and for 10% Ti to $T_{\mathrm{mag}} \simeq 25$ K. As a function of temperature, there is, to the accuracy of 10^{-3}, no shift in the peak position. The exact value of the peak position, though, varies slightly between different samples and different Ti concentrations (between 0.235 and 0.24), and there is always a significant deviation from the commensurate value $\frac{1}{4}$. Moreover, there is some indication that for the higher Ti concentration this value is larger by the order of 1%. A precise determination of the absolute magnitude of the ordered moment would require a more thorough measurement of integrated intensities on a larger set of reflections. Nevertheless we can state that the magnetic moment is quite substantial. In the scenario of a simple sinusoidal spin-density wave, we estimate it to be between 0.5 and 1 μ_B at low temperature.

Lacking suitable crystals with smaller Ti concentration, it is not possible to reliably determine the critical concentration at which magnetic order sets in; a rough extrapolation yields

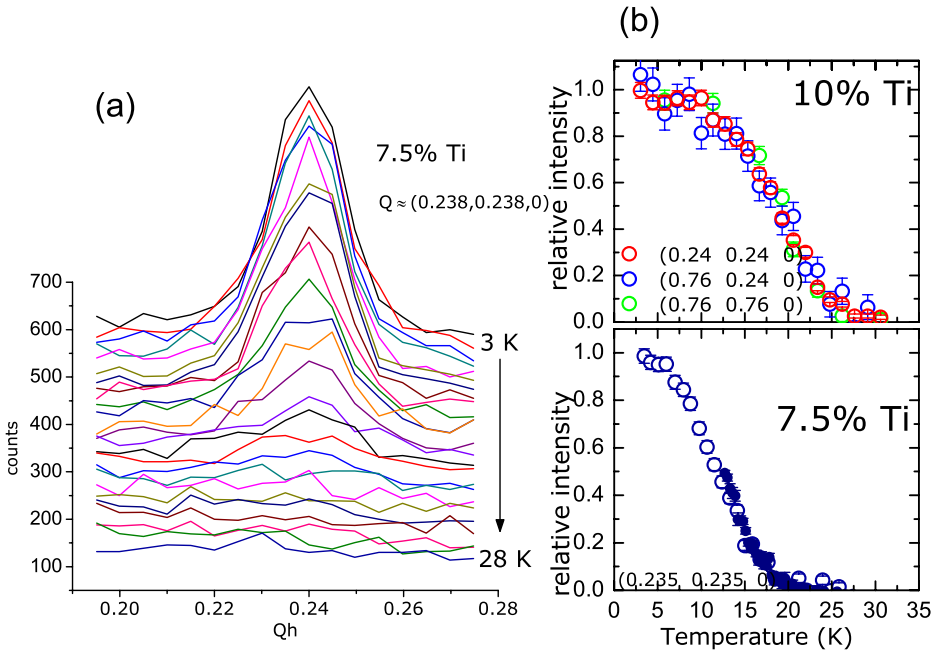

FIG. 3. (Color online) Temperature dependence of the magnetic reflections. (a) Shows transverse scan across the first magnetic reflection in $Sr_3(Ru_{0.925}Ti_{0.075})_2O_7$, and (b) summarizes the full relative temperature variation for both Ti concentrations, measured at various Q vectors.

$x_{cr-Ti} \simeq 2-4\%$ in agreement with the macroscopic measurements (see below). In the case of Mn doping,[12] the analysis of the macroscopic properties determines the critical concentration to $x_{cr-Mn} \simeq 3\%$.

It is noteworthy that the spin-density wave magnetic ordering appearing in $Sr_3(Ru_{1-x}Ti_x)_2O_7$ does not reflect the inelastic correlations detected in pure $Sr_3Ru_2O_7$.[7] In $Sr_3Ru_2O_7$ the dominant magnetic fluctuations have been observed at very different wave vectors[7] than that of the magnetic order induced by Ti doping. On the diagonal of the Brillouin zone, in particular close to $\mathbf{q_{ic}}$, no magnetic fluctuations have been reported, rendering magnetic order at this vector quite remarkable. In contrast, the magnetic order induced by Ti substitution in the single-layer material Sr_2RuO_4 appears at $\vec{q} = (0.307, 0.307, 1)$ (Ref. 15) almost exactly at the position of the strong incommensurate inelastic response of the pure material[22,26] which is very well understood in terms of Fermi-surface nesting. Pure Sr_2RuO_4 is already close to magnetic order, and upon slight Ti doping, these fluctuations finally condense into static order. In $Sr_3Ru_2O_7$ such a simple picture apparently does not hold. The transition temperatures, the size and orientation of the ordered moments, and even the two-dimensional propagation vectors are, however, remarkably similar in Ti-doped single and bilayer ruthenates, suggesting a close relation and strong similarity in the electronic structure. The in-plane correlation lengths are considerably longer in the double-layer compound as the perturbation of the magnetism due to the Ti impurity is reduced in the double-layer planes. The magnetic ordering in $Sr_3(Ru_{1-x}Ti_x)_2O_7$ for $x=7.5$ and 10% seems to be closely related with the magnetic ordering in Mn-doped $Sr_3Ru_2O_7$ where antiferromagnetic superstructure reflections were observed at the apparently inconsistent $\vec{Q} = (0.25, 0.25, 0)$ and $\vec{Q} = (0.75, 0.25, 0)$ positions by powder neutron diffraction.[12]

Magnetoelastic coupling. In the Mn-doped compounds the magnetic transition is accompanied by strong structural anomalies[12] which render it interesting to search for similar effects in the Ti-doped samples. Figure 4 shows the temperature dependence of the lattice parameters in $Sr_3Ru_2O_7$ and in $Sr_3(Ru_{0.9}Ti_{0.1})_2O_7$ determined by x-ray powder diffraction on powders obtained by crushing parts of the single crystals.[27] The RuO_6 octahedra in pure $Sr_3Ru_2O_7$ are rotated around the c axis yielding an orthorhombic symmetry with negligible orthorhombic splitting space group *Bbcb*.[28] The pure and the doped materials exhibit a negative thermal expansion coefficient along the c direction (see Fig. 4), which seems to be characteristic for layered ruthenates with a rotational distortion. In the $Ca_{2-x}Sr_xRuO_4$ series as well, the rotational distortion causes a negative c axis thermal expansion coefficient, whereas a static tilt distortion leads to a strong shrinking of the c parameter upon cooling.[29] The inclusion of the Ti into the $Sr_3Ru_2O_7$ structure causes a continuous flattening of the lattice, c shrinks, and a and b expand. The roughly constant cell volume is consistent with the idea that Ti is four-valent, but the flattening may indicate some change in the orbital occupation with respect to pure $Sr_3Ru_2O_7$.

There is no indication for any structural phase transition throughout the entire temperature range, neither in the pure nor in the substituted material (see Fig. 4). Nevertheless, a weak structural effect is observed at T_{mag}: by counting on the edge of the strong nuclear (2,0,0) Bragg-reflection profile of the $Sr_3(Ru_{0.9}Ti_{0.1})_2O_7$ single crystal on the IN22 triple-axis spectrometer, we observed a relative elongation of the in-plane lattice constant by $\sim 1 \cdot 10^{-4}$ when cooling through T_N. This effect is corroborated by the lattice-parameter studies using x-ray powder diffraction, which also indicate a flattening of the lattice in the magnetically ordered state, as well as by studies on the cold triple-axis spectrometer G4.3. In the

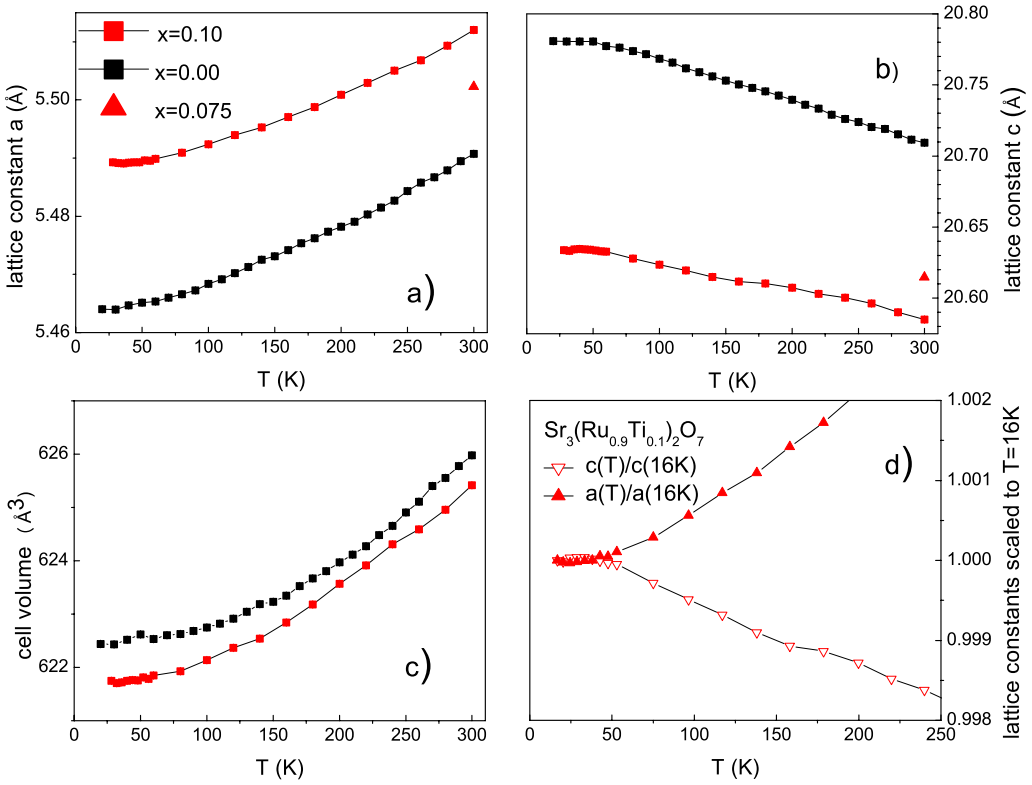

FIG. 4. (Color online) Temperature dependence of pseudotetragonal lattice parameters in $Sr_3Ru_2O_7$ and in $Sr_3(Ru_{1-x}Ti_x)_2O_7$. (a) and (b) show the a and c parameters on an absolute scale for $x=0$ and 0.10; for comparison we have included the room-temperature values for $x=0.075$. (c) presents the unit-cell volume and part (d) the lattice parameters in $Sr_3(Ru_{0.9}Ti_{0.1})_2O_7$ normalized to the low-temperature values.

related Mn-doped system,[12] $\frac{\Delta a}{a}$ amounts to about $1\cdot10^{-3}$. In the antiferromagnetic compounds $Ca_3Ru_2O_7$ and Ca_2RuO_4 the elongation $\frac{\Delta a}{a}$ amounts to $1\cdot10^{-3}$ and $1\cdot10^{-2}$, respectively.[25,29] Furthermore, the effect is also present in metallic and paramagnetic $Ca_{1.8}Sr_{0.2}RuO_4$ [and to a lesser extent at higher x in $Ca_{2-x}Sr_xRuO_4$ (Ref. 30)] $(1\cdot10^{-4})$ where it is associated with the appearance of strong inelastic antiferromagnetic correlations.[11] Thus in many layered ruthenates one observes a flattening of the lattice upon entering or approaching an antiferromagnetically ordered phase.

Any change in the octahedral environment of the Ru ions is expected to couple strongly to the 4d-orbital occupation and thereby to the orbital moments. The related magnetoelastic effects appearing in so many layered ruthenates underline the generic strong role of spin-orbit coupling.

IV. INELASTIC MAGNETIC CORRELATIONS

We have furthermore studied the magnetic excitations in $Sr_3(Ru_{0.9}Ti_{0.1})_2O_7$ by inelastic neutron scattering. As the magnetic correlations are to a large extent two dimensional, we worked around the two-dimensional zone center (1,0,0). We find an inelastic signal at $q=0.22\pm0.01$ on the a^*/b^* axes, which can be identified with the outer incommensurate $[q=(0.25,0,0)]$ signal in $Sr_3Ru_2O_7$.[7] This signal is present below and above T_N, but at 2.5 meV energy transfer χ'' decreases by a factor of ~4 when cooling from $T=33$ K to $T=1.5$ K. We could not study the inner incommensurate signal reported by Capogna *et al.*[7] as there is a strong overlapping intensity centered at the ferromagnetic zone center. In the single crystals of $Sr_3(Ru_{1-x}Ti_x)_2O_7$ other members of the Ruddlesden-Popper series, $SrRuO_3$ and $Sr_4Ru_3O_{10}$, develop as single-crystalline intergrowth phases. Due to the large ferromagnetically ordered moment of these minor impurity phases, they may imply a strong inelastic signal in spite of their low volume ratios. As in addition there is also some phonon scattering around $\vec{Q}=(1,0,0)$; we cannot reliably separate the intrinsic magnetic scattering of $Sr_3(Ru_{0.9}Ti_{0.1})_2O_7$ close to the zone center.

In contrast to pure $Sr_3Ru_2O_7$, $Sr_3(Ru_{0.9}Ti_{0.1})_2O_7$ exhibits strong fluctuations around $\mathbf{q_{ic}}$, which we have carefully studied. Figure 5 summarizes the results of momentum and energy scans for different temperatures and energy transfers. Part (a) of the figure shows excitations at temperatures below, slightly above (33 K), and far above T_N. At any temperature and energy, the signal is well described by a single Gaussian peak, without any variation in the widths.

In general, the excitation spectrum of an itinerant incommensurate antiferromagnet may have a rather complicated structure, consisting of several types of collective modes (spin waves, phason, and amplitude modes) and a continuum of excitations. The large width and the absence of dispersive features seem to suggest that the observed signals essentially reflect the excitations in the continuum, but with the present results we may not exclude that the low-energy signal at low temperatures arises from collective excitations. The spectral function at $\mathbf{q_{ic}}$ [Fig. 5(b)] exhibits a significant temperature dependence. Except at $T=1.5$ K, it can reasonably well be

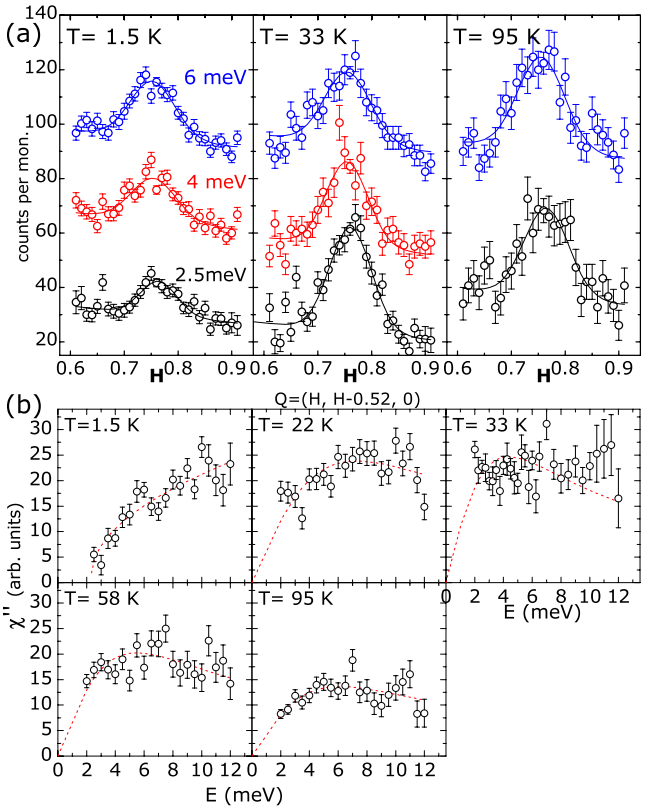

FIG. 5. (Color online) Excitations at $Q=(0.76,0.24,0)$ in $Sr_3(Ru_{0.9}Ti_{0.1})_2O_7$. (a) Shows constant energy scans along a diagonal direction in Q space for various temperatures and energy transfers (raw data; shifted by 40 counts each). (b) Shows energy scans on the peak position. By background subtraction and Bose factor correction, a quantity proportional to χ'' was obtained (lines, see text).

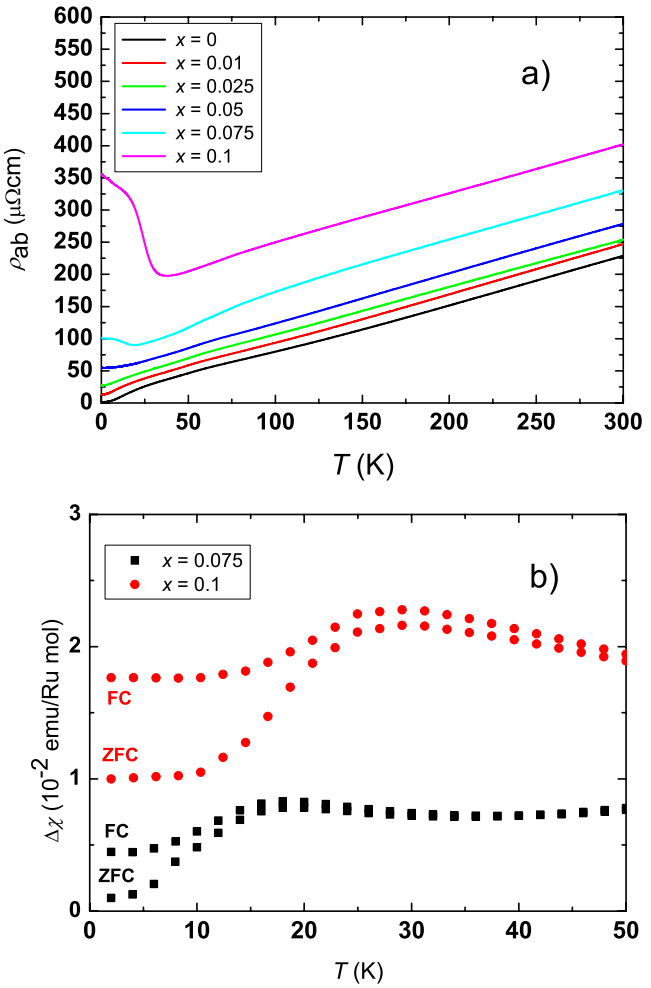

FIG. 6. (Color online) (a) In-plane resistivity in $Sr_3(Ru_{1-x}Ti_x)_2O_7$ for a wide range of Ti concentrations as a function of temperature. (b) Magnetic susceptibility, $\Delta\chi$, of $Sr_3(Ru_{1-x}Ti_x)_2O_7$ for $x=0.075$ and 0.10 after subtracting the contributions of $SrRuO_3$ and $Sr_4Ru_3O_{10}$ impurity phases; field-cooled (FC) and zero-field-cooled (ZFC) data were obtained with the magnetic field parallel to c; the upper curves were shifted for clarity.

described by a single-relaxor function,[31] $\chi''(\omega)=\chi_0'\cdot\omega\Gamma/(\omega^2+\Gamma^2)$, with an amplitude χ_0' (real part of χ at $\omega=0$) and a characteristic energy Γ. As expected, the amplitude increases when approaching the magnetic transition, where, however, only one component, χ_c, should diverge.[32] At $T=22$ K, i.e., slightly below T_N, the spectral weight at low energy is already reduced compared to $T=33$ K, and at $T=1.5$ K there is a clear gap in the excitation spectrum of about 2 meV. Taking account of the magnetic transition temperature in the framework of weak-coupling theory,[33] one estimates the gap of the excitation continuum to a significantly higher value:$2\Delta\simeq 3.5k_BT_N\simeq 7.5$ meV. The low-energy excitations observed at low temperature should be close to the crossover between magnon and continuum features, and anisotropy terms should play an important role. A comprehensive study of the magnetic excitations in the ordered states of the doped $Sr_3Ru_2O_7$ compounds appears highly interesting.

The observed magnetic fluctuations are qualitatively similar to the ones in $V_{2-x}O_3$, one of the very few systems with an incommensurate spin-density wave ground state that have been studied by inelastic neutron scattering.[34,35] The magnetic excitations in $Sr_3(Ru_{0.9}Ti_{0.1})_2O_7$ furthermore resemble those observed in the single-layer Ti-doped Sr_2RuO_4.[15] The spin dynamics in the lower energy range should contain interesting and qualitatively different features such as collective modes, but these would probably be difficult to detect, and the effects of disorder introduced by the chemical doping might be detrimental.

V. MACROSCOPIC MEASUREMENTS

The macroscopic properties further confirm the spin-density wave magnetic ordering in $Sr_3(Ru_{1-x}Ti_x)_2O_7$. The in-plane resistivity in $Sr_3(Ru_{0.9}Ti_{0.1})_2O_7$ exhibits an upturn upon cooling at $T_{mag}=25$ K (see Fig. 6(a)]. This resistivity increase on the order of $\Delta\rho_{ab}\simeq 150$ $\mu\Omega$ cm (Ref. 23) is, however, small compared to the corresponding increase by about 2 orders of magnitude at the magnetic ordering in $Sr_3(Ru_{0.9}Mn_{0.1})_2O_7$.[12] $Sr_3(Ru_{0.925}Ti_{0.075})_2O_7$ also exhibits a smaller resistivity upturn at T_{mag}, but samples with lower concentration do not show a clear feature in the resistivity. Nevertheless the small Ti contents significantly alter the resistivity. For Ti concentrations between 0% and 4% the re-

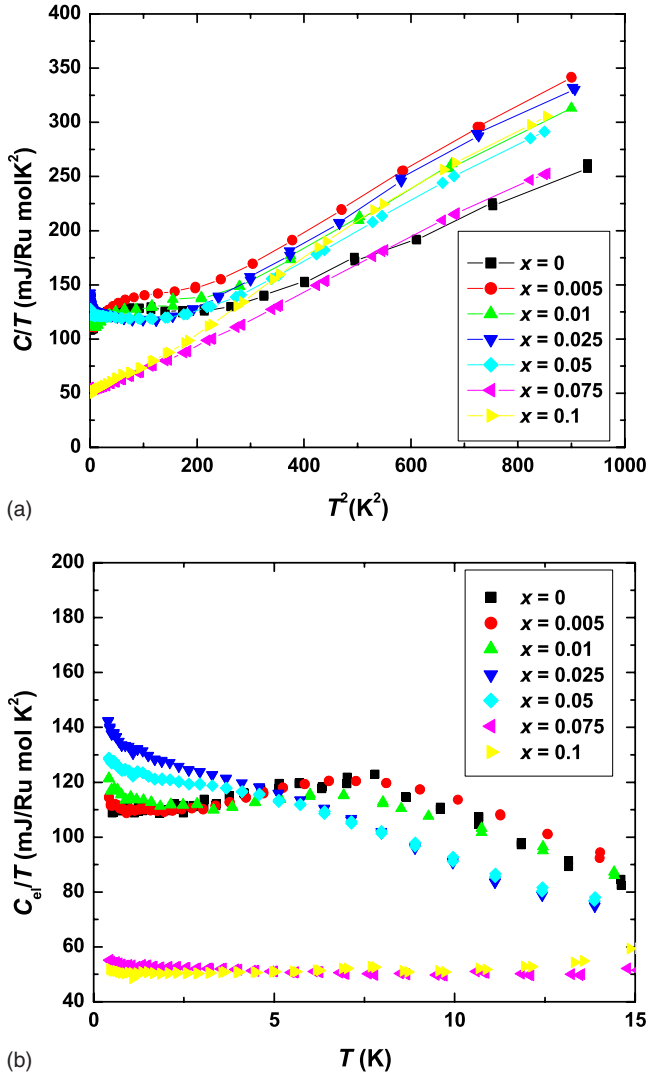

FIG. 7. (Color online) Specific heat in $Sr_3(Ru_{1-x}Ti_x)_2O_7$ for a wide range of Ti concentrations. In the upper part we show $\frac{C_p}{T}$ as a function of T^2, and in the lower part we show the electronic part of $\frac{C_p}{T}$ versus T after subtraction of the parabolic phonon contribution.

sistivity decreases when cooling from 10 to 0.5 K, whereas it increases for contents larger than 5%,[13] suggesting the critical concentration to be around $x_{cr-Ti} \simeq 4\%$.

Pure $Sr_3Ru_2O_7$ exhibits a maximum in the temperature dependence of the magnetic susceptibility which is characteristic for a metamagnetic material. This maximum is rapidly suppressed by the Ti doping.[13] Furthermore, the signature of the metamagnetic transition in the magnetization versus magnetic field curves disappears for a Ti content of 4% in the crystals studied in Ref. 13 as well as in our crystals. At Ti contents of 3% and 4% the c axis magnetic susceptibility continuously increases upon cooling, exceeding the in-plane values, and the two samples with $x=0.075$ and $x=0.1$ exhibit pronounced differences between field and zero-field cooling [see Fig. 6(b) and Ref. 23]. These findings support the alignment of the ordered magnetic moments along the c direction as determined by the neutron-diffraction studies: The nonmagnetic substitution creates a finite moment in the spin-density wave, which can be aligned by the field. The resistivity and the susceptibility in the two samples which exhibit the spin-density wave ordering agree remarkably well with the observations in the Ti-doped Sr_2RuO_4 series.[14,15]

Hooper *et al.*[13] presented low-temperature specific-heat data for $Sr_3(Ru_{1-x}Ti_x)_2O_7$ with $x=0.0$, 0.005, and 0.04. The maximum of the $\frac{C_p}{T}$ data in pure $Sr_3Ru_2O_7$ is suppressed already by 0.5% of Ti, and the low-temperature limit of $\frac{C_p}{T}$ in the $x=0.04$ sample is about 30% larger than that in $Sr_3Ru_2O_7$. We have extended the specific-heat measurement to the larger Ti-concentration range (see Fig. 7), which allows us to relate the specific heat with the magnetic fluctuations. In accordance with the detailed studies on $Ca_{1.8}Sr_{0.2}RuO_4$,[11,30] we interpret the maximum of the specific heat in the pure compound by the suppression of ferromagnetic fluctuations in zero field at low temperature. The increase in the low-temperature limit of $\frac{C_p}{T}$ upon increasing the Ti can be ascribed to the softening of the magnetic fluctuations near $\mathbf{q_{ic}}$ close to the transition which has been observed in the neutron experiment as a function of temperature. The maximum in the $\frac{C_p}{T}$ low-temperature limit indicates a critical concentration of the spin-density wave ordering around 4% of Ti. At higher concentrations in the static spin-density wave phase, the $\frac{C_p}{T}$ coefficient gets effectively suppressed due to the opening of the gap in the spin excitations which is seen in the inelastic neutron-scattering spectra. The strength of the $\frac{C_p}{T}$ suppression is remarkable and indicates that the gap in the magnetic fluctuations or the hardening of the fluctuations is not limited to $\mathbf{q_{ic}}$ but possesses considerable weight throughout the Brillouin zone. The absence of a clear anomaly in the specific-heat data may be ascribed to the sluggish character of the magnetic transition which corresponds to a crossover from two-dimensional to three-dimensional ordering.

VI. CONCLUSIONS

The magnetic ordering in Ti-doped $Sr_3Ru_2O_7$ has been characterized by elastic and inelastic neutron-scattering studies. $Sr_3(Ru_{1-x}Ti_x)_2O_7$, with Ti concentrations of 7.5 and 10%, exhibits an incommensurate spin-density wave magnetic ordering with a propagation vector of $\mathbf{q_{ic}}=(0.24,0.24,0)$. It is remarkable that the magnetic ordering does not reflect a pronounced inelastic magnetic correlation already present in pure $Sr_3Ru_2O_7$. In contrast, in the single-layer ruthenates, Ti doping leads to a condensation of the dominant magnetic instability of pure Sr_2RuO_4. In $Sr_3(Ru_{1-x}Ti_x)_2O_7$ there is a ferromagnetic coupling within the two layers of a bilayer and the ordered moment points along the c axis. The correlation length is long in the basal plane and short along the c direction reflecting the weak magnetic coupling between the bilayers. The in-plane correlation length of about 40 lattice spacings by far exceeds the mean Ti-Ti distance indicating that the impurities perturbate the magnetic correlations less than in the single-layer material. Signatures of the spin-density wave magnetic ordering are seen in the resistivity, in the magnetic susceptibility, and in the specific heat, although only the resistivity exhibits a well-defined anomaly at the magnetic transition.

Strong magnetic excitations at $\mathbf{q}_{ic}$ are associated with this magnetic instability. Their spectral weight increases upon cooling toward the transition, and a gap develops below T_{mag}. These magnetic excitations constitute an additional component to the reported excitation spectrum of $Sr_3Ru_2O_7$ in contrast to the case of the single-layer compounds where Ti doping leads to the condensation of the dominating magnetic instability in the pure material.[15,22] Further experiments are required to clarify the relation between the distinct magnetic instabilities in pure and Ti-doped $Sr_3Ru_2O_7$. The softening of magnetic fluctuations at $\mathbf{q}_{ic}$ and the opening the gap in the ordered phase are reflected in the doping and temperature dependencies of the specific heat.

ACKNOWLEDGMENTS

This work was supported by the Deutsche Forschungsgemeinschaft through Grant No. SFB 608 and by the UK EPSRC-GB through the Portfolio Partnership "Novel Quantum Ordering in the Correlated Electron Materials." We thank J. Brand for a measurement of lattice parameters.

*Present address: Institut Laue Langevin, Grenoble, France; steffens@ill.eu

†braden@ph2.uni-koeln.de

[1] R. S. Perry, L. M. Galvin, S. A. Grigera, L. Capogna, A. J. Schofield, A. P. Mackenzie, M. Chiao, S. R. Julian, S. Ikeda, S. Nakatsuji, Y. Maeno, and C. Pfleiderer, Phys. Rev. Lett. **86**, 2661 (2001).

[2] A. J. Millis, A. J. Schofield, G. G. Lonzarich, and S. A. Grigera, Phys. Rev. Lett. **88**, 217204 (2002).

[3] S. A. Grigera, R. Perry, A. Schofield, M. Chiao, S. Julian, G. Lonzarich, S. Ikeda, Y. Maeno, A. Millis, and A. Mackenzie, Science **294**, 329 (2001).

[4] R. S. Perry, K. Kitagawa, S. A. Grigera, R. A. Borzi, A. P. Mackenzie, K. Ishida, and Y. Maeno, Phys. Rev. Lett. **92**, 166602 (2004).

[5] S. A. Grigera, P. Gegenwart, R. A. Borzi, F. Weickert, A. J. Schofield, R. S. Perry, T. Tayama, T. Sakakibara, Y. Maeno, A. G. Green, and A. P. Mackenzie, Science **306**, 1154 (2004).

[6] K. Kitagawa, K. Ishida, R. S. Perry, T. Tayama, T. Sakakibara, and Y. Maeno, Phys. Rev. Lett. **95**, 127001 (2005).

[7] L. Capogna, E. M. Forgan, S. M. Hayden, A. Wildes, J. A. Duffy, A. P. Mackenzie, R. S. Perry, S. Ikeda, Y. Maeno, and S. P. Brown, Phys. Rev. B **67**, 012504 (2003).

[8] M. B. Stone, M. D. Lumsden, R. Jin, B. C. Sales, D. Mandrus, S. E. Nagler, and Y. Qiu, Phys. Rev. B **73**, 174426 (2006).

[9] S. Ramos, E. M. Forgan, C. Bowell, S. M. Hayden, A. J. Schofield, A. Wildes, E. A. Yelland, S. P. Brown, M. Laver, R. S. Perry, and Y. Maeno, Physica B **403**, 1270 (2008).

[10] O. Friedt, P. Steffens, M. Braden, Y. Sidis, S. Nakatsuji, and Y. Maeno, Phys. Rev. Lett. **93**, 147404 (2004).

[11] P. Steffens, Y. Sidis, P. Link, K. Schmalzl, S. Nakatsuji, Y. Maeno, and M. Braden, Phys. Rev. Lett. **99**, 217402 (2007).

[12] R. Mathieu, A. Asamitsu, Y. Kaneko, J. P. He, X. Z. Yu, R. Kumai, Y. Onose, N. Takeshita, T. Arima, H. Takagi, and Y. Tokura, Phys. Rev. B **72**, 092404 (2005).

[13] J. Hooper, M. H. Fang, M. Zhou, D. Fobes, N. Dang, Z. Q. Mao, C. M. Feng, Z. A. Xu, M. H. Yu, C. J. O'Connor, G. J. Xu, N. Andersen, and M. Salamon, Phys. Rev. B **75**, 060403(R) (2007).

[14] M. Minakata and Y. Maeno, Phys. Rev. B **63**, 180504(R) (2001).

[15] M. Braden, O. Friedt, Y. Sidis, P. Bourges, M. Minakata, and Y. Maeno, Phys. Rev. Lett. **88**, 197002 (2002).

[16] K. Pucher, J. Hemberger, F. Mayr, V. Fritsch, A. Loidl, E. W. Scheidt, S. Klimm, R. Horny, S. Horn, S. G. Ebbinghaus, A. Reller, and R. J. Cava, Phys. Rev. B **65**, 104523 (2002).

[17] S. V. Halilov, D. J. Singh, J. Minar, A. Y. Perlov, and H. Ebert, Phys. Rev. B **71**, 100503(R) (2005).

[18] S. Ray, D. D. Sarma, and R. Vijayaraghavan, Phys. Rev. B **73**, 165105 (2006).

[19] M. Abbate, J. A. Guevara, S. L. Cuffini, Y. P. Mascarenhas, and E. Morikawa, Eur. Phys. J. B **25**, 203 (2002).

[20] K. W. Kim, J. S. Lee, T. W. Noh, S. R. Lee, and K. Char, Phys. Rev. B **71**, 125104 (2005).

[21] J. Kim, J.-Y. Kim, B.-G. Park, and S.-J. Oh, Phys. Rev. B **73**, 235109 (2006).

[22] Y. Sidis, M. Braden, P. Bourges, B. Hennion, S. NishiZaki, Y. Maeno, and Y. Mori, Phys. Rev. Lett. **83**, 3320 (1999).

[23] J. Farrell, Ph.D. thesis, University of St. Andrews, 2007.

[24] M. K. Crawford, R. L. Harlow, W. Marshall, Z. Li, G. Cao, R. L. Lindstrom, Q. Huang, and J. W. Lynn, Phys. Rev. B **65**, 214412 (2002).

[25] Y. Yoshida, S.-I. Ikeda, H. Matsuhata, N. Shirakawa, C. H. Lee, and S. Katano, Phys. Rev. B **72**, 054412 (2005).

[26] M. Braden, Y. Sidis, P. Bourges, P. Pfeuty, J. Kulda, Z. Mao, and Y. Maeno, Phys. Rev. B **66**, 064522 (2002).

[27] For comparison we also show the lattice parameters for pure $Sr_3Ru_2O_7$ measured on a sample provided by Perry *et al.* (Ref. 4).

[28] H. Shaked, J. D. Jorgensen, O. Chmaissem, S. Ikeda, and Y. Maeno, J. Solid State Chem. **154**, 361 (2000).

[29] O. Friedt, M. Braden, G. André, P. Adelmann, S. Nakatsuji, and Y. Maeno, Phys. Rev. B **63**, 174432 (2001).

[30] M. Kriener, P. Steffens, J. Baier, O. Schumann, T. Zabel, T. Lorenz, O. Friedt, R. Müller, A. Gukasov, P. G. Radaelli, P. Reutler, A. Revcolevschi, S. Nakatsuji, Y. Maeno, and M. Braden, Phys. Rev. Lett. **95**, 267403 (2005).

[31] T. Moriya, *Spin Fluctuations in Itinerant Electron Magnetism* (Springer-Verlag, Berlin, 1985).

[32] M. Braden, P. Steffens, Y. Sidis, J. Kulda, P. Bourges, S. Hayden, N. Kikugawa, and Y. Maeno, Phys. Rev. Lett. **92**, 097402 (2004).

[33] P. Fazekas, *Lecture Notes on Electron Correlation and Magnetism* (World Scientific, Singapore, 1999).

[34] W. Bao, C. Broholm, S. A. Carter, T. F. Rosenbaum, G. Aeppli, S. F. Trevino, P. Metcalf, J. M. Honig, and J. Spalek, Phys. Rev. Lett. **71**, 766 (1993).

[35] W. Bao, C. Broholm, G. Aeppli, S. A. Carter, P. Dai, T. F. Rosenbaum, J. M. Honig, P. Metcalf, and S. F. Trevino, Phys. Rev. B **58**, 12727 (1998).